Cement and Concrete Research 41 (2011) 1244–1256

Contents lists available at ScienceDirect

Cement and Concrete Research

journal homepage: http://ees.elsevier.com/CEMCON/default.asp

Supplementary cementitious materials

Barbara Lothenbach [a,*], Karen Scrivener [b], R.D. Hooton [c]

[a] Empa, Laboratory for Concrete & Construction Chemistry, CH-8600 Dübendorf, Switzerland
[b] EPFL, Laboratory of Construction Materials, CH-1015 Lausanne, Switzerland
[c] University of Toronto, Dept. of Civil Engineering, Toronto, Canada, M5S 1A4

ARTICLE INFO

Article history:
Received 1 October 2010
Accepted 1 December 2010

Keywords:
Blended cements [D]
Supplementary cementitious material [D]
Thermodynamics [B]
Hydrates [B]
Kinetic [C]

ABSTRACT

The use of silica rich SCMs influences the amount and kind of hydrates formed and thus the volume, the porosity and finally the durability of these materials. At the levels of substitution normally used, major changes are the lower Ca/Si ratio in the C–S–H phase and consumption of portlandite. Alumina-rich SCMs increase the Al-uptake in C–S–H and the amounts of aluminate containing hydrates. In general the changes in phase assemblages are well captured by thermodynamic modelling, although better knowledge of the C–S–H is needed.
At early ages, "filler" effects lead to an increased reaction of the clinker phases. Reaction of SCMs starts later and is enhanced with pH and temperature. Composition, fineness and the amount of glassy phase play also an important role. Due to the diverse range of SCM used, generic relations between composition, particle size, exposure conditions as temperature or relative humidity become increasingly crucial.

Contents

* Corresponding author.
E-mail address: barbara.lothenbach@empa.ch (B. Lothenbach).

0008-8846/$ – see front matter
doi:10.1016/j.cemconres.2010.12.001

1. Introduction

Today supplementary cementitious materials (SCMs) are widely used in concrete either in blended cements or added separately in the concrete mixer. The use of SCMs such as blast-furnace slag, a byproduct from pig iron production, or fly ash from coal combustion, represents a viable solution to partially substitute Portland cement (PC). The use of such materials, where no additional clinkering process is involved, leads to a significant reduction in CO_2 emissions per ton of cementitious materials (grinding, mixing and transport of concrete use very little energy compared to the clinkering process) and is also a means to utilize by-products of industrial manufacturing processes.

Most of the available studies on the properties of blended systems focus on mechanical or durability aspects of a specific fly ash or slag. Our knowledge about fundamental connections between the overall composition and the hydrates formed as well as their impact on the long-term development of such systems is insufficient. The main processes taking place in the hydration of Portland cements (PC) are well known (see e.g. the comprehensive book of Taylor [1]). The clinker phases hydrate at various rates resulting mainly in the formation of C–S–H, portlandite, ettringite and AFm phases. The blending of SCMs with Portland cement leads to a more complicated system where the hydration of the Portland cement and hydraulic reaction of the SCM occur simultaneously and may also influence the reactivity of each other. The reaction of most SCMs is slower than the reaction of the clinker phases and difficult to follow as many SCMs consist of X-ray amorphous glasses. The kinetics of the SCM reaction depends on the chemical composition, the fineness, and on the amount of reactive phases such as glass or zeolites of the SCM used as well as on the composition of the interacting solution. Comparatively little is known about the detailed effect of these parameters due to the difficulty to measure the reaction of SCMs quantitatively in blended systems.

In this paper the effects of SCMs on microstructure and hydration kinetics are reviewed. Based on numerous papers on the subject an attempt was made to identify underlying principles based on chemistry and thermodynamics, including also new and unpublished works from the authors, which illustrate these aspects.

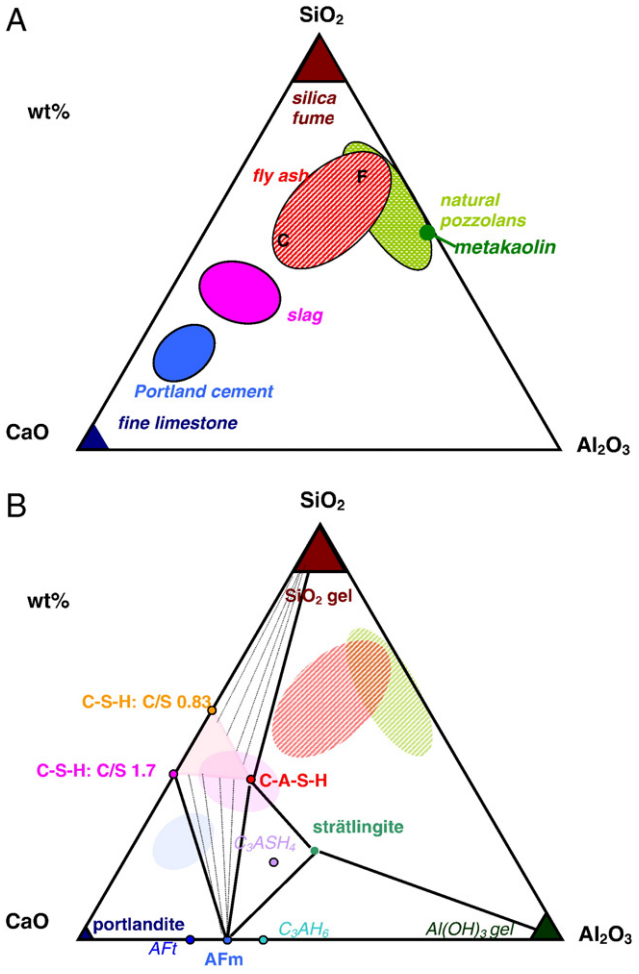

Fig. 1. A) $CaO–Al_2O_3–SiO_2$ ternary diagram of cementitious materials, B) hydrate phases in the $CaO–Al_2O_3–SiO_2$ system. Note that in the absence of carbonate or sulfate, C_3AH_6 will be more stable than the AFm phases.

Table 1
Average chain length of Portland cement (PC) with metakaolin (MK).

	Average chain length	Al/Si
100% PC	2.62	0.043
80% PC + 20% MK	4.38	0.103
70% PC + 30% MK	7.24	0.149

2. Phase assemblages and thermodynamic modelling

The chemistry of supplementary cementitious materials is generally characterized (with the notable exception of fine limestone, which is not discussed further here) by lower calcium content than Portland cement (Fig. 1A). Thus there are differences in the hydrates formed during hydration, which influence strength and durability. Fig. 1B shows schematically the hydrate phases formed in the $CaO–SiO_2–Al_2O_3$ system. One striking feature of this diagram is the large field of compositions of the C–S–H phase, which is the most important phase in cements. It is well established, that the C–S–H in systems containing silica-rich SCMs is significantly different to C–S–H in Portland cements. At Ca/Si ratios >1.5 C–S–H might be described by disordered jennite-like units $(CaO)_{1.5–1.9}SiO_2\cdot(H_2O)_x$ [2,3] or a tobermorite structure with calcium hydroxide-like regions.[1] At lower Ca/Si ratios, a tobermorite-like structure $(CaO)_{0.83}SiO_2\cdot(H_2O)_{1.5}$) with defects in the silicate "dreierketten" chains has been proposed [2,3]. For C–S–H incorporating aluminium, "C–A–S–H", a tobermorite-like structure seems to be maintained [4]. The incorporation of aluminium in C–S–H increases with increasing aluminium concentration in the solution [4] and with increasing Si/Ca ratio of the C–S–H [2]. The boundaries shown in Fig. 1 are only an approximation as the limits of the possible solid solutions are not well known, particularly with respect to the amount of alumina which can be incorporated.

Qualitatively it can be seen, that blending of PC with silica fume (Fig. 1) will lead to a decrease of the amount of portlandite and the formation of more C–S–H with a lower C/S ratio. Similarly, blending of PC with fly ash will decrease the amount of portlandite, increase the amount of C–S–H with a lower Ca/Si and the amount of AFm phases as fly ash can contain high quantities of Al_2O_3. Blending with blast-furnace slag has little effect on the amount of portlandite with respect to clinker, until high level of substitution. However, more C–S–H with a lower Ca/Si will be formed to accommodate the lower overall Ca/Si ratio of the system.

Depending on the composition and the reactivity of the SCM, also the amount of ettringite and the amount and kind of AFm phases such as monosulfate, monocarbonate or strätlingite are affected. This is illustrated below for silica fume, fly ash and slag composite cements.

[1] There is considerable controversy as to whether high C/S ratio C–S–H is based on a disordered jennite structure or a tobermorite-like structure with calcium hydroxide type regions (or even something in between). It is beyond the scope of this paper to enter into this debate. In this paper we use the expression "jennite-like" as this has conventionally been used in thermodynamic modeling.

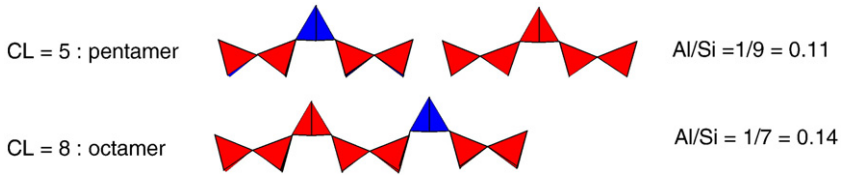

Fig. 2. Schematic representation of the average chain length and the Al-uptake by bridging tetrahedra.

2.1. Characteristics of C–S–H in blended cements

The C–S–H present in Portland cement has a composition of ~1.5–1.9$CaO \cdot SiO_2 \cdot nH_2O$. The number n of water molecules depends on relative humidity and temperature. The addition of silica-rich SCMs results in the formation of a C–S–H with lower C/S, which is generally agreed to have a tobermorite-like structure ($(CaO)_{0.83}SiO_2 \cdot (H_2O)_{1.5}$) but with many defects, mainly in positions of the bridging silicon tetrahedron (see footnote 1). The fraction of such defects determines the mean silica chain length, which is measurable e.g. by ^{29}Si NMR [5,6]. The average chain length increases as the C/S ratio decreases [5,6].

The formation of C–S–H with a low C/S leads to an increased uptake of aluminum [2] in the C–S–H: C–A–S–H. Aluminium enters C–S–H mainly at the bridging sites in the silicate chains [2,7]. Table 1 illustrates these points for mixes containing metakaolin from an unpublished study by Minard [8]. Fig. 2 shows a graphic representation of the silicate chains corresponding to these figures. In both cases of metakaolin addition, the Al/Si ratio implies that roughly one in two of the bridging sites are occupied by aluminium. Similar or even higher Al/Si ratios were reported in the literature for other aluminium-rich SCMs, e.g. for 30% fly ash blends hydrated at 55 °C by Girão et al. [9].

Many researchers speak about C–S–H from the hydration of Portland cement and "pozzolanic" C–S–H from the reaction of blended systems as though these are distinguishable products. However, the evidence indicates that the composition of the C–S–H tends to even out. Rims of different grey level, may be observed around the SCM particles, but these differences are mainly due to high levels of intermixing with other phase, such as aluminium-containing phases [10] or, notably in the case of slag, with a hydrotalcite-like phase containing magnesium and aluminium [10–12]. Particularly at low degrees of reaction of the SCM it is still possible to distinguish the "inner product" rims of dense, homogeneuous C–S–H around the clinker grains from the more porous "outer" product between the clinker and the SCM grains. For example Kocaba [13] found the composition of C–S–H in blended Portland cement–slag systems was relatively homogenous (Figs. 3 and 4). The dark rims around the slag particles visible in Fig. 3 are due to the high amounts of hydrotalcite-like phase concentrated within these rims due to the low mobility of magnesium. Fig. 4 shows the average $Ca/(Si+Al)$ values. After 28 days when about 30–40% of the slag has reacted, the average $Ca/(Si+Al)$ value had dropped from close to 2 for the reference pure Portland cement to between 1.5 and 1.6. After one year, this ratio is below 1.5. Then it is no longer possible to distinguish between inner product around the cement grain and the outer products, Fig. 3.

2.2. PC–silica fume

Silica fume consists nearly exclusively of SiO_2 of very fine particle size and a relatively high pozzolanic activity. Thus the PC–silica fume system is most appropriate to illustrate the effect of silica-rich material on the phase assemblage in Portland composite cements using thermodynamic calculations (Fig. 5; more details in Appendix A). These calculations treat the high Ca/Si ratio "jennite" like C–S–H, and lower Ca/Si ratio "tobermorite" like C–S–H as separate phases for convenience, even though they cannot be distinguished microstructurally as discussed above.

In a completely hydrated Portland cement containing calcite, jennite-like C–S–H, portlandite, ettringite, monocarbonate and a hydrotalcite-like phase are the main hydrates that form (e.g. [1,14], left side of Fig. 5). According to the thermodynamic calculations, an addition of moderate amounts of SiO_2 leads to the consumption of portlandite as visible in Fig. 5. If even more silica fume is added, the surplus SiO_2 reacts with the high calcium C–S–H ("jennite-like" C–S–H: $(CaO)_{1.67}(SiO_2)_1 \cdot (H_2O)_{2.1}$) to progressively more low calcium C–S–H ("tobermorite-like" C–S–H: $(CaO)_{0.83}(SiO_2)_1 \cdot (H_2O)_{1.3}$). Low Ca/Si C–S–H can incorporate more aluminium in its structure than high Ca/Si C–S–H [2,4]. For the calculations a constant $Al/Si = 0.05$ for jennite- and tobermorite-like C–S–H has been used.

The formation of low Ca/Si C–S–H with Al will lead to a decrease of dissolved calcium and an increased uptake of alkalis [15,16], and thus to a reduction of alkali concentration and pH in the pore solution [17–20], with the latter resulting in the destabilization of monocarbonate (Fig. 5). The calculations indicate that as soon as the pH of the pore solution would fall below 10 due to further replacement of PC by silica fume, also the ettringite would become unstable.

The hydrate assemblage observed experimentally in SiO_2–PC blends agrees well with the modelling results shown in Fig. 5. It consists of mainly C–S–H, ettringite, AFm phases [20–22] and a reduced quantity of portlandite [22–25]. The blending of PC with ≥24 wt.% silica fume resulted after longer hydration times in the entire consumption of portlandite with ettringite and C–S–H with a reduced Ca/Si ratio as the only hydrate phase observed ([22,23,25,26], Fig. 6). As the silica fume continued to react, the low pH values and the absence of portlandite destabilized the monocarbonate with time [26,27]. The calculations in Fig. 5 indicate, that upon further replacement of PC by silica fume (or upon further reaction of the silica fume), ettringite will become unstable. The dissolution of

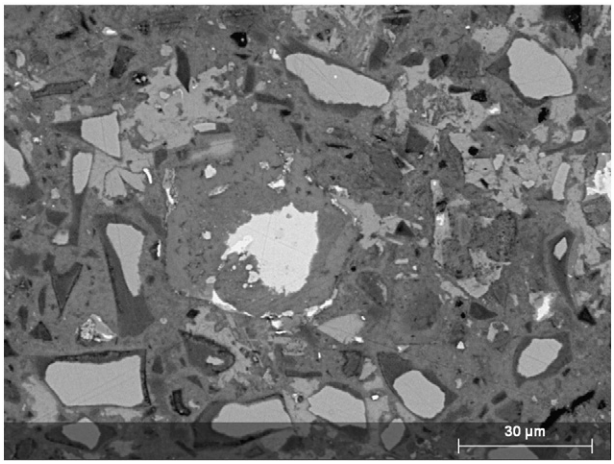

Fig. 3. SEM-BSE from a 60% Portland cement–40% slag blend (B-S1) hydrated for 1 year. From Kocaba [13].

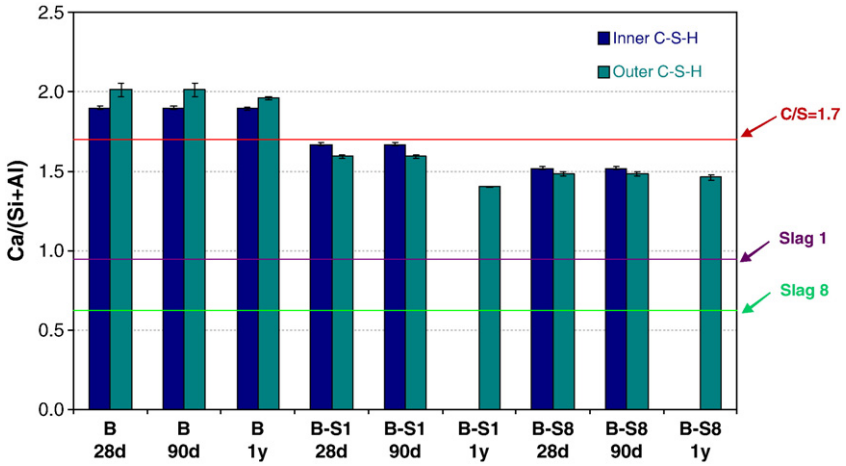

Fig. 4. Ca/(Si + Al) ratio in Portland cement (B) and 60% Portland cement–40% slag blends (B-S1; B-S8) hydrated up to 1 year. The lines indicate the Ca/(Si + Al) ratio of the pure slags (slags 1 and 8).
From Kocaba [13].

ettringite has been observed in binary (60% Portland cement, 40% silica fume) or ternary blends (37.5% Portland cement, 32.5% silica fume and 30% fly ash) with high hydration degrees or under leached conditions [20,28]. However, gypsum was not observed to precipitate, the sulphate ions remaining partly in the interstitial solution, and partly sorbed onto C–S–H.

Fig. 5 illustrates an important aspect related to the partial replacement of Portland cement with SCMs — the decrease in the total volume of hydrates formed. This should mean that blended pastes have higher total porosities than pure PC pastes. This seems paradox as it is well established that PC–SCM blends can develop higher strengths and lower permeabilities than plain PC pastes (e.g. [29]). This poses the question as to whether the effective density, or space filling capacity of C–S–H in blended pastes is the same as in plain Portland pastes. Measurements indicate that blended systems show often equal or even higher total porosities than pure PC pastes, but a refined pore structure [30–33]. In particular, slag-PC pastes have been observed to contain more fine pores and less coarse capillary pores than PC pastes, resulting in a reduced permeability [30,32].

2.3. PC–fly ash

Fly ashes consist mainly of SiO_2, but can contain also significant quantities of Al_2O_3. The amount of CaO is limited but highly variable depending on the origin of the fly ash (e.g. [1], Fig. 1). The ASTM C618 standard differentiates high calcium Class C-fly ashes and low-calcium Class F ashes. As the latter are the most abundant, the following discussion focuses on Class F fly ash. The blending of Portland cement with fly ash results in the reduction of the total amount of portlandite in the hydrated mixture, somewhat less pronounced than for silica fume as (i) the reactivity of fly ash is very limited and (ii) as the CaO in the fly ash is an additional source of calcium. Class F fly ashes contain between 15 and 35% alumina, so the blending of PC with such fly ash results in high amounts of Al-rich phases. As systematic information about the Al-uptake by C–S–H are still missing (see also discussion in Appendix A), the high aluminium content in the system, coupled with a potentially high aluminium uptake in C–S–H introduces a considerable error in the thermodynamic calculations. For our calculations, a constant Al/Si of 0.1 in C–S–H was assumed. The results indicate, in the presence of moderate amounts of fly ash, the destabilization of

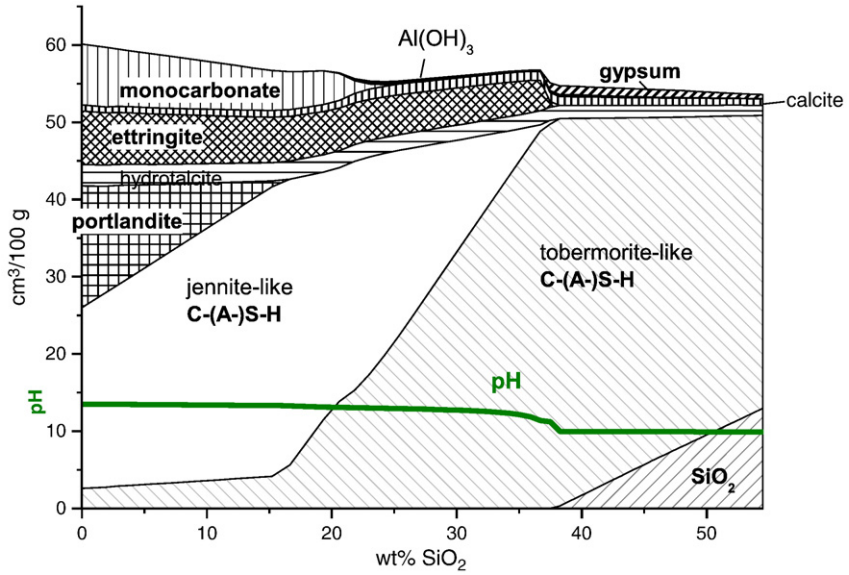

Fig. 5. Modelled changes in hydrated Portland cement upon blending with SiO_2, assuming complete reaction of the Portland cement (CaO 60, SiO_2 22, Al_2O_3 4.6, Fe_2O_3 2.7, MgO 1.9, Na_2O 0.3, K_2O 1.0, SO_3 3.2, CO_2 2 wt.%) and SiO_2.

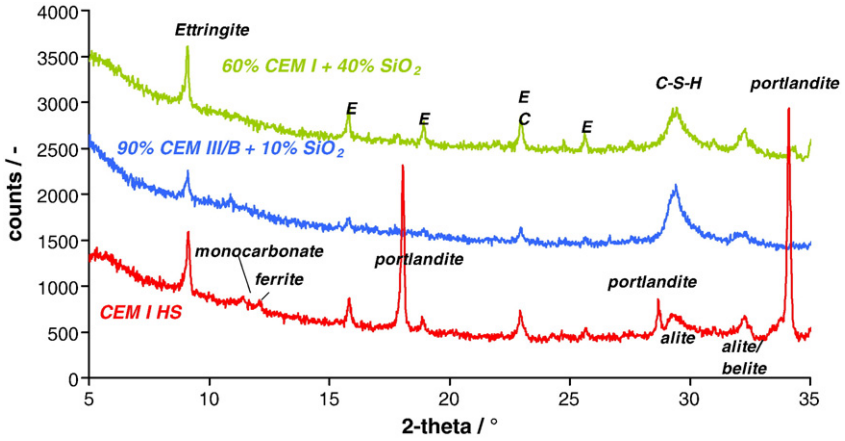

Fig. 6. Phase composition observed by XRD in a hydrated Portland cement, a CEM III/B blended with 10% SiO_2 and a CEM I blended with 40 wt.% SiO_2 after one year of hydration. Graph modified from [26].

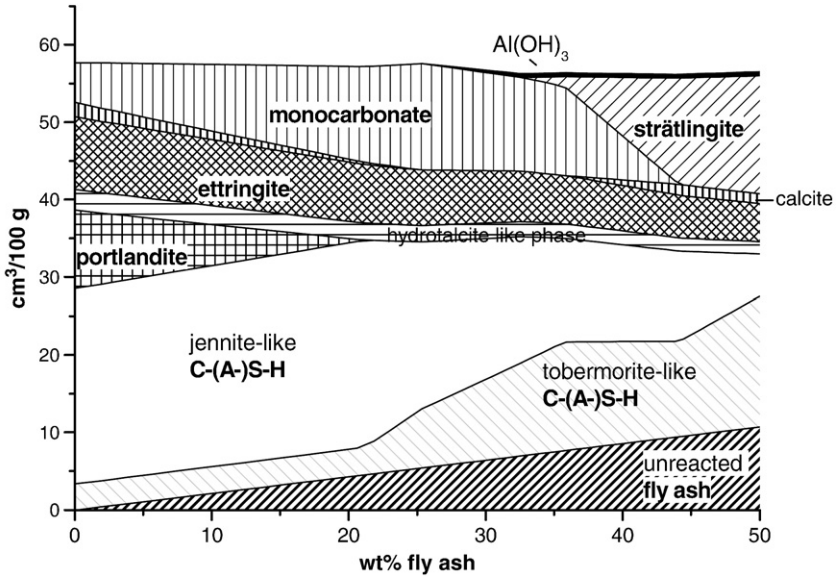

Fig. 7. Modelled changes in hydrated Portland cement upon blending with fly ash, assuming complete reaction of the Portland cement (CaO 60, SiO_2 22, Al_2O_3 4.6, Fe_2O_3 2.7, MgO 1.9, Na_2O 0.3, K_2O 1.0, SO_3 3.2, and CO_2 3 wt.%) and 50% reaction of a low Ca fly ash (CaO 4.4, SiO_2 54, Al_2O_3 31, Fe_2O_3 4.6, MgO 0.8, Na_2O 0.6, K_2O 0.8, and SO_3 0.4 wt.%).

portlandite and the formation of additional C–S–H with a decreased Ca/Si ratio (Fig. 7). As fly ashes contain significant quantities of Al_2O_3 but little SO_3,[2] the blending of PC with fly ash results in a decrease of ettringite and in an increase of AFm content. The addition of further $CaSO_4$ would increase the fraction of ettringite formed, resulting in a higher total volume of the hydrates. Above 40% of fly ash in the cement, monocarbonate and eventually ettringite are calculated to become unstable. Strätlingite may form if high quantities of Al-rich fly ash are used (Fig. 7). The calculations indicate that the formation of strätlingite depends on the reactivity of the fly ash, the amount of Al_2O_3 present in the fly ash and on the uptake of Al in C–S–H.

The calculated phase changes in Fig. 7 agree with experimental observations. For ≥60% replacement of Portland cement by fly ash, the complete depletion of portlandite has been observed after hydration times of 1 year and longer [34,35]. After 1 year and longer, when a significant amount of the fly ash has reacted, a decrease of the amount of ettringite (due to the high Al_2O_3 and low SO_3 content of fly ashes) and an increase of the amount of AFm phases like monosulfate or monocarbonate [10,36–39] has been observed. Also the presence of strätlingite [10,37,40] has been reported. The C–S–H formed in PC–FA blends has a lower Ca/Si ratio and contains more Al [10,38,41–43]. However, in contrast to the thermodynamic modelling results, the presence of strätlingite has been observed in systems where portlandite is also present, e.g. by Escalante-Garcia and Sharp [10] for a one year old 70–30 wt.% PC–FA blend suggesting that the different hydrate assemblages calculated in Fig. 7 may be present at the same time but in different places of the microstructure of PC–fly ash blended cements.

2.4. PC–slag

Granulated blast-furnace slag (gbfs) contains more CaO but significantly less Al_2O_3 than fly ash (Fig. 1). Calculations of the influence of the stable phase assemblage of PC blended with gbfs give results similar to silica fume and fly ash blended systems: destabilization of portlandite but, due to the higher CaO content, only at high replacement levels (Fig. 8), the formation of C–S–H with a lower C/S, the disappearance of monocarbonate. Whether strätlingite is predicted or not depends on the Al-content of the gbfs and on the uptake of Al in C–S–H. Gbfs contain typically 7–15 wt.% MgO; thus the thermodynamic calculations predict the formation of more hydrotalcite-like solids than for silica fume or fly ash systems.

[2] When SCMs are blended with clinker at the cement plant the SO_3 content is usually adjusted to optimise strength development. Such additions will clearly impact the conclusions from thermodynamic calculation.

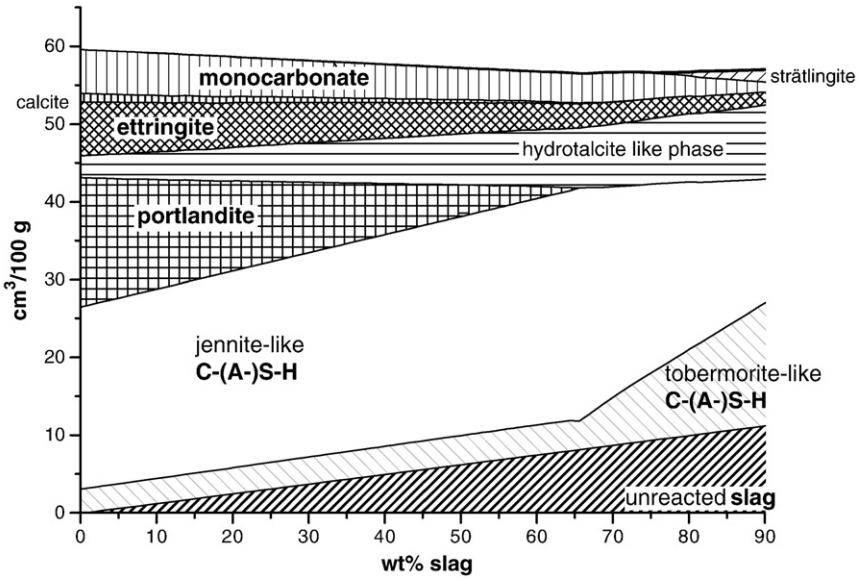

Fig. 8. Modelled changes in hydrated Portland cement upon blending with blast furnace slag, assuming complete reaction of the Portland cement (CaO 60, SiO_2 22, Al_2O_3 4.6, Fe_2O_3 2.7, MgO 1.9, Na_2O 0.3, K_2O 1.0, SO_3 3.2, and CO_2 3 wt.%) and 75% reaction of a blast furnace slag (CaO 39, SiO_2 38, Al_2O_3 11, Fe_2O_3 1, MgO 10, K_2O 0.3, and S 1 wt.%). Al/Si in C–S–H = 0.1.

Thermodynamic calculations published by Atkins et al. [44] for PC–slag systems, assuming complete hydration of the slag and the PC, gave comparable results; they predicted the absence of portlandite in blended systems with a high percentage of blast furnace slag, the formation of C–S–H with a lower C/S ratio, the presence of a hydrotalcite-like phase and AFm phases including strätlingite. It should be borne in mind that generally gbfs does not fully hydrate as evidenced by residual slag grains found even in 20 years old cements [12,38].

Published experimental investigations agree with the thermodynamic modelling (Fig. 8). Experimentally the presence of portlandite, C–S–H, ettringite, AFm (monosulfate and monocarbonate), and a hydrotalcite-like phase has been observed in hydrated PC–slag systems [10,12,13,20,21,35,38,42,45]. At longer hydration times less portlandite than in pure Portland cements is found [12,13,20,38,42,45,46]. High gbfs content have been observed to lead to presence of less ettringite [12]. Even though blast furnace slags contain more Al_2O_3 than PC, which could potentially lead to more AFm and AFt phases in the PC — gbfs composites, generally less AFm and AFt phases than in pure PC are observed [12,13,37,38], as more Al is bound in the C–S–H [12,13,42,47,48]. The C–S–H formed in PC–slag blends has a lower Ca/Si ratio and a higher Al/Si ratio than pure PC ([10,12,13,38,42,47,48], Fig. 4).

3. Kinetics

The understanding of the reaction kinetics in blended systems is complicated by the fact that the hydration of the clinker and SCM may interact and, more importantly, by the difficulty in measuring the degree of reaction of these two components independently. For these reasons there is little quantitative data available on the rate of reaction of supplementary cementitious materials.

3.1. Filler effect

It has been realized for a long time, notably by Gutteridge [49,50], that even inert materials blended with cement may have a significant effect on the hydration of the clinker phases. This is usually referred to as a filler effect. However, the reactivity of SCMs themselves is often confused with this filler effect. The reactivity of most SCMs is highly dependent on the alkalinity of the pore solution, which builds up over the first few days. Consequently the amount of reaction of SCMs in the first day or so is usually negligible and changes in hydration kinetics are dominated by the filler effect. This is particularly evident in the case of silica fume, which generally enhances mechanical properties even at one day, despite the fact that ^{29}Si NMR indicates almost no reaction of silica fume at this stage [27,51,52].

There seem to be two principal mechanisms contributing to the filler effect:

- Extra space: As the filler does not produce hydrates, at the same water to *solids* ratio, the water to *clinker* ratio is higher and there is more space for the hydration products of the clinker phases.
- Enhanced nucleation: Particularly for fine materials, the extra surface provided by the SCMs acts as nucleation sites for the hydration products of the clinker phases.

Recent results from Fernandez [53] and Kocaba [13] illustrate these effects. Figs. 9 and 10 show the heat evolution curves for blends with quartz filler and silica fume compared to reference cements. In both cases the heat evolution is normalized to the amount of clinker phases present. Quartz was chosen as a nominally inert material, although there may be some reaction of an amorphized surface layer

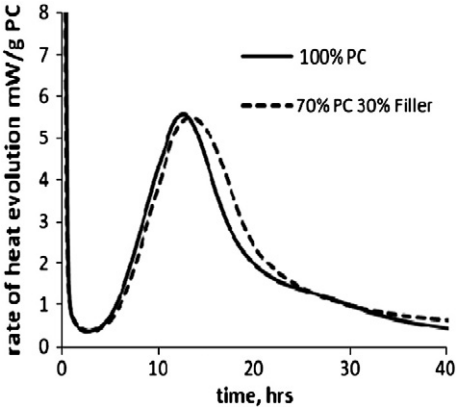

Fig. 9. Hydration of 100% PC compared to 70% PC with 30% fine quartz filler. The rate of heat evolution is normalised to the PC content [53]. The quartz, as it does not react significantly, gives more space for hydration product of the PC so the acceleration period is prolonged.

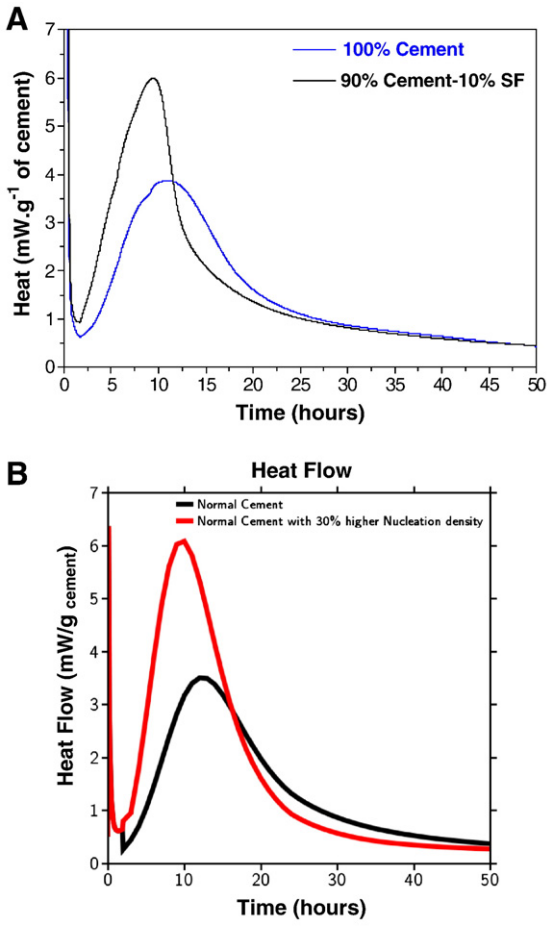

Fig. 10. a) 100% PC compared to 90% PC with 10% silica fume, the fine particles of silica fume act as nucleation sites to give a steeper acceleration and higher maximum rate of heat evolution [56]. Panel b shows simulation results in which the number of nucleation sites increased by 30% [57].

formed during grinding. In the case of quartz it is seen that there is almost no impact on the slope of the heat evolution curve during the acceleration period. However the acceleration period is extended, with the maximum heat evolution occurring later. As discussed in another paper in this volume [54] nucleation and growth control the reaction kinetics well beyond the heat peak maximum and the maximum corresponds to impingement of hydration products. In the model of Bishnoi [55], where the filling of space can accounted for explicitly, it seems the deceleration period starts when C–S–H growing out from the cement grains in a diffuse manner, with low packing density encounters products from a neighbouring grain. The observations of the impact of inert fillers on the silicate reaction shown in Fig. 9 support this hypothesis.

In the case of silica fume, Fig. 10A, there is clearly another effect. The increase in heat evolution during the acceleration period is much steeper. The heat maximum is much higher. This effect on the acceleration and deceleration periods is consistent with an increase in the number of nucleation sites as shown in the simulation in Fig. 10B.

It seems that nucleation effects may be even more marked in the case of the hydration products of the aluminate phase, which normally gives rise to a second or shoulder peak in calorimetry after the main peak associated with the hydration of alite. Fig. 11 shows the hydration of a cement alone and with the addition of various fillers, none of which are expected to react [58]. Similar nucleation effects have also been observed for carbon black particles [59]. The additions of the fine materials; corundum and rutile, have a slight impact on the silicate reaction as described above, but the impact on the aluminate reaction is much more significant. The aluminate peak is sharpened, becoming narrower and higher.

Similar effects on the aluminate peak have been reported for Portland cement slag blends and several researchers have attributed the more significant peak to an early reaction of the slag itself [10,60,61]. Kocaba [13] used a technique of progressive additions of gypsum and peak deconvolution to quantify the energy emitted in this peak for plain Portland pastes and blends with slag. Within the limits of the precision of the method it appears that the amount of reaction (of the C_3A phase) is the same in both cases. This suggests that fillers and SCMs promote the nucleation of the hydrates forming during this aluminate reaction, rather than react themselves. Although filler effects have been widely noted, and are clearly significant, there have not really been any systematic investigations of the critical parameters, such a particle size, crystallography, etc. and such work is clearly important in the future to better understand the impact of supplementary cementitious materials.

3.2. Techniques to measure the reaction of SCMs

As already indicated, our understanding of the reaction kinetics of SCMs is hampered by the difficulty in measuring independently the degree of reaction of the SCMs and clinker phases, which is complicated by the presence of the filler effects as described above.

The most widely used technique to assess the degree of reaction of plain Portland cements is evaluation of the bound water content from the weight loss of samples dried to 105° and then fired to 1000 °C. Despite the various stochiometries of the reactions of the various clinker phases, it is usually found that the average values of bound water per gram of reacted material are similar for different Portland cements. However, the situation becomes much more complicated when SCMs are used and this method cannot be used to separate the reaction of the SCM from the reaction of the clinker phases.

The technique which has been used most widely to try and measure the reactions of SCMs in blended systems is selective dissolution [62]. The intention of such methods is that the unreacted clinker phases and the hydrates from the clinker and slag reaction are dissolved, leaving only the unreacted slag or fly ash as a residue. Study of residues by X-ray diffraction and SEM reveals that significant amounts of clinker and hydrate phases remain after dissolution [13,62–64]. It is claimed that the effects of incomplete dissolution can be corrected for. However, recent independent work by two of the authors of this paper [13,63–65] indicates that large, non-quantifiable systematic errors remain as different assumptions lead to large differences in the quantity of FA or slag reacted. This probably explains why different authors report very different amounts of slag

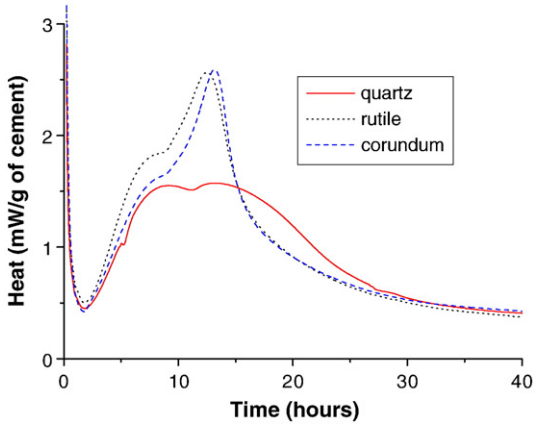

Fig. 11. Heat evolution for PC blended with corundum, rutile or quartz. Fineness: corundum 5.4 $m^2\ g^{-1}$; rutile 9.1 $m^2\ g^{-1}$; quartz 0.76 $m^2\ g^{-1}$.
Adapted from [58].

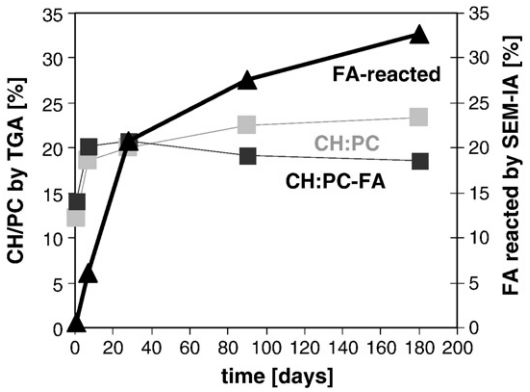

Fig. 12. Portlandite (CH) content and degree of fly ash (FA) reaction in a PC and a 65% PC–35% FA paste.
Data from [69].

reaction in similar systems. For example, Escalante et al. [46], find degrees of reaction of about 20% after 3 months compared to values of around 40% reported by Luke and Glasser [62] and Lumley et al. [66].

The reaction of fly ash and silica fume was often followed by the decrease of the amount of portlandite in the mixture [22,23,25,45,67,68]. This fast and easy method is well suited to assess that an increasing fraction of the SCM reacts with time (Fig. 12). However, quantitative determinations of the fraction of SCM reacted are not possible as the reaction of the clinkers might be accelerated due to filler effect and as the silica fume or fly ash reaction might lead, even in the presence of portlandite, to the formation of low Ca/Si C–S–H. During the first days of hydration more portlandite may be observed in a Portland cement–fly ash paste than in a pure PC, if the CH content is normalised to the amount of clinker (Fig. 12). Only after 28 days and longer less portlandite is present indicating a reaction of the fly ash. In contrast, the reaction of fly ash as determined by SEM-image analysis points out a continuing reaction of the fly ash.

Image analysis of flat polished sections imaged with backscattered electrons has proven to be a very useful technique to measure the degree of reaction of clinker phases [70,71]. This has the advantage that it can also be used to study the reaction of the clinker phases in blended systems (Fig. 12). This method can also be developed to study the degree of reaction of slag and even fly ash [13,63–65,69,72,73]. The close similarity in grey levels between some slags and calcium hydroxide mean that this technique may require consideration of images of elemental distributions for X-ray microanalysis. The main drawback of this technique is that it is very time consuming and has relatively low precision in the range of 2–4%.

A quantitative determination of the amount of silica fume reacted can be obtained by using the broad Q^4 peak characteristic for amorphous SiO_2 in ^{29}Si MAS NMR [22,51,52,74–77]. ^{29}Si MAS NMR is also useful to follow the amount of silicate reacted from other SCMs. ^{29}Si MAS NMR has been used to quantify the degree of slag reacted [12,76,78,79] and very recently also of fly ash [76,77,79] in blended systems. In some cases it had to be combined with selective extraction techniques as the overlap of peaks of C–S–H and slag caused deconvolution problems [78]. The use of NMR in PC–fly ash systems is generally hindered by the line broadening caused by the too high iron content of the fly ash. The main limitations of this technique are the limited availability of the equipment, the need for specialists for interpretation of the results and its time consuming nature (one ^{29}Si spectrum may take one day to acquire). Furthermore, if the SCMs contain too much iron the technique may be unusable.

A promising technique, which allows continuous monitoring of an SCM is comparison of the cumulative calorimetry or chemical shrinkage curves for a blend of Portland cement with SCM, compared to a blend of the same Portland cement with a quartz filler ground to a similar particle size distribution to the SCM [13,65,69]. As shown in Fig. 13 this gives results which correlate very well with measures from image analysis. The current problem with this technique is the lack of information on the specific heat evolution or chemical shrinkage to relate the data obtained to degree of reaction. Clearly more work is needed on calibration and optimisation of the filler materials, but, nevertheless, the technique seems promising.

The measurement of the rate of reaction of SCMs in blended systems is hampered by the lack of fast, reliable and precise methods. Many values can be found in the literature for individual SCMs, but the scatter of results and the diversity of methods and materials used mean that only general trends can be identified as discussed below. However a good quantitative understanding of the rate of reaction and parameters affecting this is still needed.

3.3. Influence of different factors on reaction rate

3.3.1. Composition of the SCM

Each SCM has a different range of chemical compositions. For a given pH and temperature, the solubility of the resulting glassy phases will vary. In addition, high-calcium fly ashes typically also contain reactive crystalline phases, such as tricalcium aluminate, di-calcium silicate and free lime, which both accelerate and increase the complexity of the hydration reactions.

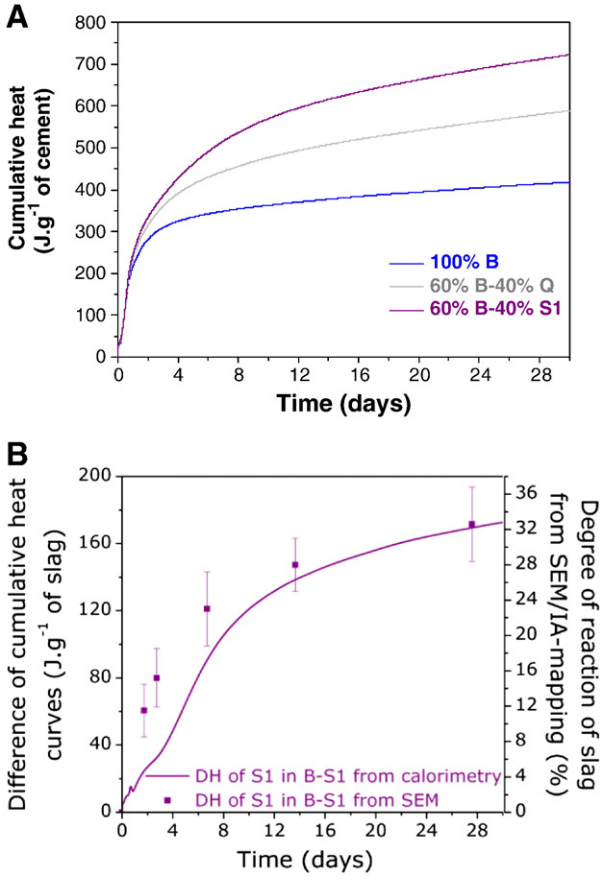

Fig. 13. Calorimetry methods to monitor the reaction of slag continuously in Portland cement (B) and 60% Portland cement–40% slag or quartz blends (B-S1; B-Q). To eliminate the filler effect, the paste of the cement plus slag is compared to a mixture of the same cement with the same substitution of quartz filler ground to the same size as the slag. A) Cumulative heat. B) Difference between the cumulative curves for the slag blend and the filler blend (left *y*-axis) compared to measurements of degree of reaction from image analysis (right *y*-axis).
From [13,65].

3.3.2. Replacement level

Due to different levels of reactivity of different types of SCMs, for sufficient rates of reaction required to attain equivalent strengths, replacement levels are different. For example, 20% low-calcium fly ash, 35% slag, 4% silica fume and 10% metakaolin might be expected to provide similar 28-day strengths in concrete cured at 20 °C (e.g. [19,80]). While early-age strengths might be reduced, higher levels of SCM may be required to attain special performance, such as control of alkali–silica reaction (ASR), increased chloride penetration resistance, sulfate resistance (e.g. >65% gbfs for high SR), or lower heat of hydration (e.g. >50% slag or >30% fly ash). Due to extremely high surface areas, silica fume and metakaolin will increase rates of reaction, in part due to nucleation effects (silica fume) and in part due to pozzolanic reaction. However, at excessive replacement rates, reaction rates are reduced due to reduced pH resulting from the rapid early rates of reaction.

3.3.3. Solution pH

The solubility of amorphous silica is extremely sensitive to increases in pH between 12 and 14. The higher the pH, the faster the rate of reaction [81,82]. In Portland cement–SCM blends, the high pH is provided by alkali hydroxides and calcium hydroxide, with pore solution pH increasing rapidly in the first few hours of hydration as sulfate ions are removed from pore solution due to reaction with aluminates. To maintain electro-neutrality, hydroxyl ions replace the sulfate ions in solution, and pH levels are usually maintained between 13 and 14 after about 24 h [83,84]. These hydroxyl ions allow the secondary reactions to occur with the amorphous silica-rich phases in SCMs. Provided that sufficient hydroxyl ions remain in solution to maintain the pH of the pore solution, the SCM reactions will continue. If the SCM replacement level is too high, the pH will drop, reducing the solubility of the amorphous silicates and thus slowing the rate of reaction.

3.3.4. Temperature

Both pozzolanic and the latent hydraulic slag reaction rates are typically more sensitive to temperature [22,34,52,85], reacting more slowly than Portland cements at temperatures below about 15 °C but rates are often accelerated at temperatures above 27 °C, usually associated with hot-weather concreting. This temperature sensitivity often limits practical cement replacement levels in cool weather, but allows higher replacement levels in warm weather.

3.4. PC–silica fume

The reactivity of silica fume (SF) is generally larger than the one of slag or fly ash [45] due to its small particle size. However, measurements of the relative decrease of the amount of portlandite due to the pozzolanic reaction and ^{29}Si MAS NMR indicate a rather slow reaction of the silica fume in blended systems continuing for months [45,51,52,75,77]. ^{29}Si NMR indicates relatively little reaction (~5%) of silica fume during the first hours in PC–SF mixtures, while afterwards the reaction rate is strongly increased, so that 20 to 80% of the silica fume have reacted after 2 days or longer [27,51,77,86]. As the pH in the pore solution of PC pastes increases strongly after approx. 12 to 16 h (e.g. [83,84]), the reaction of the silica fume is then accelerated. At later ages, the additional C–S–H formed by the reaction of the silica fume takes up alkalis, decreasing the pH of the pore solution [67,87] so that the further reaction of the silica fume slows down. Similarly, high replacement of PC by silica fume decreases the reaction of silica fume [21,52] as the pH of the pore solution decreases. However, even in the absence of portlandite, silica fume continues to react, but more slowly [22]. At higher temperatures the reaction of the silica fume proceeds faster [22,52,85,88].

3.5. PC–fly ash

The reaction of fly ash is slow at ambient temperatures and only after longer hydration times (≥1 week), the quantity of portlandite relative to the amount of Portland cement is reduced [34,37,89–92]. Initially, the amount of portlandite compared to pure PC, increases slightly [34,45,89,90] (Fig. 12), as the hydration of the clinker is accelerated due to the filler effect thus producing more portlandite. This slow reaction of the fly ash is the reason that the hydrate assemblage of Portland cement–fly ash blends is initially identical to the pure Portland cement system: C–S–H, portlandite, ettringite, and AFm phases like monocarbonate or monosulfate [21,36,39]. High quantities of FA slow down the reaction [34,90], while higher temperatures [34] accelerate the reaction of fly ash considerably.

3.6. PC–slag

Generally, slags show a faster reaction than fly ashes. The fraction of slag reacted after a specific time increases if less slag is present in the blend [12]. As for other SiO_2-rich materials the reactivity of slag decreases with decreasing pH and thus with less PC present in the blended system. During the first hours or days of hydration, however, the amount of portlandite (relative to Portland cement) is in blended PC–slag systems similar or even higher than in pure Portland cements [13,45,46] due to faster reaction of the clinkers caused by the filler effect. In the long term generally a small to moderate reduction of the amount of portlandite (relative to Portland cement) is observed [13,37,45,46].

4. Liquid phase

4.1. Changes in pore solution composition

The blending of Portland cement with silica fume lowers the alkali and hydroxide concentrations in the pore solution significantly [17,67,93]. Once portlandite is depleted, the calcium concentration is also reduced. The same effect can also be observed for Portland systems blended with low-calcium fly ash [67,94–98]. High calcium fly-ash systems have been observed to exhibit pH values in the range of 12–13, with relatively low alkali concentration but higher alumina concentrations than Portland cement systems [40]. However, some Class C fly ashes can have very high alkali contents and thus increase the pH compared to PC [99]. The blending of PC with SCM rich in silica and poor in alkalis, leads to a reduction of the pH and the alkali concentrations in the pore solutions as (i) the Portland cement is diluted, (ii) the portlandite is consumed by the pozzolanic reaction leading to lower Ca concentration in the pore solution and (iii) as C–S–H with a lower Ca/Si ratio and higher alumina content leads to an increase in alkali uptake by C–S–H [15,16]. The higher sorption of alkalis by low Ca/Si C–S–H is probably caused by the negative charges due to the ionisation of silanol groups, the partial substitution of Si(IV) by Al(III) and the lower concentrations of calcium. The increased uptake of alkalis by the low Ca/Si C–S–H leads to a reduction in pore solution alkalinity far in excess of that resulting from simple dilution of the Portland cement alkalis [40,67,87,95,96].

In Portland cements blended with slags, an additional effect lowers the pH values of the pore solution. Not only the dilution of the PC and the increased uptake of alkali by the low Ca/Si C–S–H, but also the high concentrations of negatively charged soluble sulfur species lower the pH. The reducing conditions in blast furnace slags lead to the presence of reduced sulfur species such as sulfide (HS^-), sulfite (SO_3^{2-}) and thiosulfate ($S_2O_3^{2-}$) in the pore solutions [93,95,100–102]. High concentrations of these negatively charged soluble sulfur species lower the dissolved hydroxide concentrations and thus the pH in the

pore solution significantly as the electroneutrality of the solution has to be maintained.

4.2. Long-term alkalinity

The reduction of the alkali concentration and the pH of the pore solution of blended cements is found to reduce alkali silica reaction (ASR) and the resulting expansion. Whether blending merely delays ASR or prevents it, depends on the long-term pore solution alkalinity. In blends with silica fume, where no additional alumina is present in the pozzolan, the alkalis are reduced due to initial hydration reactions, but their concentrations slowly increase over time [67,87]. The reductions in alkalinity remain stable (i.e. alkalis are not released over time) when alumina-bearing SCMs such as fly ash are used [67,87], possibly due to the formation of alumina-substituted C–A–S–H. These differences in alkali concentration also lead to differences in long-term expansion, as confirmed by the continuing expansion of silica fume blended specimen containing up to 10% of silica fume [18,103], while slag or fly ash blends are more effective in reducing expansion also in the long term.

Fly ashes can have a wide variety of calcium and alkali contents, and this has been found to influence their ability to reduce alkalinity and to mitigate deleterious ASR expansions [18,98]. For fly ashes of different compositions, the alkalis released from the PC–SCM system increase as the calcium and alkali contents of the blends increased and their silica content decrease [99]. Ternary blends containing silica fume and fly ash also show superior performance in terms of binding and retaining alkalis, even though silica fume on its own does not retain alkalis in the C–S–H over time.

5. Summary and perspectives

The presence of SCMs influences the amount and kind of hydrates formed in cementitious systems and thus the volume, the porosity and finally the durability of such systems. At the levels of substitution normally used, the major change is in the composition of the C–S–H phase which moves to lower Ca/Si ratios, despite the fact that portlandite is still present in most systems. For SCMs containing alumina the C–S–H also incorporates a considerable amount of this element. In addition to the changes in C–S–H, the amounts of aluminate-containing hydrates may increase and when the SCM contain magnesium, a hydrotalcite-like phase may appear. In general the changes in phase assemblages may be well captured by thermodynamic modelling, although better knowledge of the limits of solid solution of C–S–H (particularly with regard to the uptake of aluminium) is needed.

As a consequence of the changes in phase assemblages, and particularly the changes in C–S–H, the pore solutions in blended systems differ from those in pure Portland materials. The main tendency is to lower levels of pH. This is very beneficial to avoid alkali silica reaction.

The effect of SCMs on reaction kinetics is complicated by the interaction between the clinker phases and the SCMs. At early ages “filler” effects dominate, leading to increased, and sometimes also faster, reaction of the clinker phases, due more space relative to the amount of clinker and increased nucleation rates. The hydration of the aluminate phases, which occurs after the main silicate hydration peak is often more sensitive to nucleation effects.

The reactions of SCMs themselves are difficult to measure, although promising new methods are being developed. Because of this, we do not at present have a detailed quantitative understanding of the parameters affecting reaction rate. However general trends are clear: The reaction of SCMs (including silica fume) only starts after the first day or so, when the pH of the pore solution rises due to consumption of sulfate and release of alkalis by reaction of the clinker phases, however the lower Ca/Si ratio C–S–H may adsorb alkalis, contributing to a reduction in reaction rate over time. The particle size of the SCM is clearly important as the reaction takes place at the surface, fine materials react faster. The composition of the glassy materials also plays a role, but a good appreciation of this is lacking. A very important parameter is also the temperature. Higher temperatures greatly accelerate the rate of reaction of SCM. However, again, although disparate information exists in the literature, we do not currently have a good quantitative understanding of the effects of temperature.

It is clear that the effects of SCMs on reaction kinetics is a field where more systematic study is needed. The increasingly diverse range of supplementary materials used (and proposed for use) in cementitious materials highlights the need for generic, quantitative relations between composition, particle size and other characteristics on the one hand and exposure conditions such as temperature and relative humidity on the other in order to predict the evolution of phases assemblages and microstructure.

Acknowledgements

This paper is an outcome of the International Summit on Cement Hydration Kinetics and Modeling. The authors acknowledge financial support from Nanocem for the work of Vanessa Kocaba, from the Swiss National Science Foundation (snf) for the study of Rodrigo Fernandez Lopez and Aditya Kumar, from COIN (COncrete INnovation centre) for the study of Klaartje De Weerdt and from Nagra (Swiss National Cooperative for the Disposal of Radioactive Waste) for the experimental work on low alkali cements. The authors would like to thank also Gwenn Le Saout, Luigi Brunetti, Helen Minard, Jorgen Skibsted and Mohsen Ben Haha for their support and helpful discussions.

Appendix A. Thermodynamic modelling

Thermodynamic modelling or also mass balance calculations can be used to predict the stable phase assemblage based on the composition of the starting materials. Changes in the overall chemical composition of the anhydrous system affect the amount as well as the kind of hydrates that will form. The simplest way to calculate the composition of a hydrated cement is to do mass balance calculations based on the chemical composition of the unhydrated cement [104,105]. These calculations have the advantage that they can be carried out simply with a calculator, but also the disadvantage that the possible stable phase assemblage has to be known a priori. The use of thermodynamic calculations allows the prediction of the hydrate composition also in less well-known systems, easy and fast parameter variations and thus the systematic study of the effects of changes in the composition of the starting materials or in temperature [14,106,107].

A.1. Basics of thermodynamic modelling

The thermodynamic calculations in this paper were carried out using the Gibbs free energy minimization program GEMS [108]. GEMS is a broad-purpose geochemical modelling code which computes equilibrium phase assemblage and speciation in a complex chemical system from its total bulk elemental composition. Chemical interactions involving solids, solid solutions, and aqueous electrolyte are considered simultaneously. The speciation of the dissolved species as well as the kind and amount of solids precipitated are calculated. The thermodynamic data for aqueous species, gaseous phases as well as for many solids were taken from the PSI-GEMS thermodynamic database [109,110]. Solubility products for cement minerals including ettringite, different AFm phases, hydrogarnet, C–S–H and hydrotalcite were taken from the cemdata07 compilation [106,111]. The formation of siliceous hydrogarnet has been excluded due to its slow kinetic of formation in all the calculations shown in this paper.

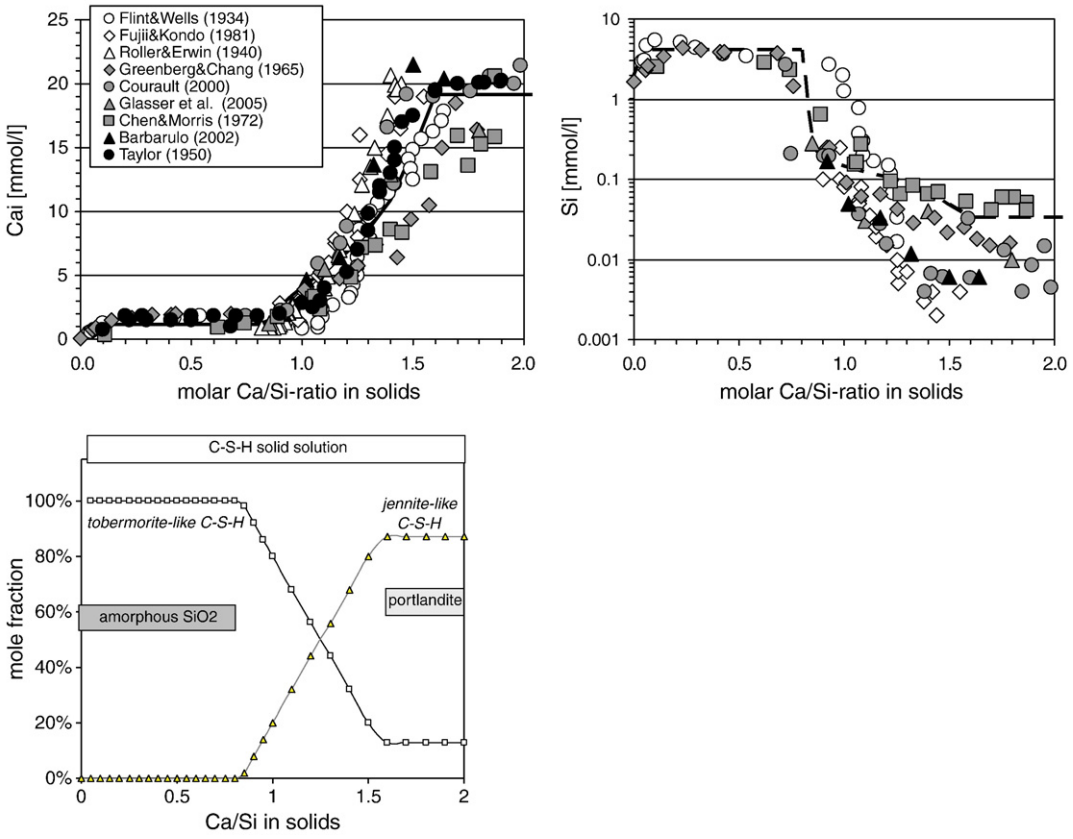

Fig. A1. Aqueous concentrations and mole fractions of the C–S–H solid solution end-members (jennite–tobermorite) as a function of the Ca/Si ratio. The presence of portlandite and amorphous SiO_2 is indicated by horizontal lines (out of scale). Modified from [84,106].

A.2. C–S–H

Due to its variable composition, C–S–H shows an incongruent solubility behaviour upon decalcification. Dissolved calcium and silicon concentrations vary with the calcium to silica ratio (C/S) of the solid and with pH. A number of experimental investigations studied the solubility of synthetic C–S–H and give a dataset to describe the solubility of C–S–H as a function of the Ca/Si ratio (see Fig. A1). In this paper, C–S–H phases are modelled using the solid solution model originally developed by Kulik and Kersten [112,113] and later adapted by Lothenbach et al. [106]. The C–S–H system is described by an ideal solid solution with the end-members jennite $(CaO)_{1.67}(SiO_2)_1\cdot(H_2O)_{2.1}$ and tobermorite $(CaO)_{0.83}(SiO_2)_1\cdot(H_2O)_{1.3}$. The uptake of aluminium by the C–S–H is simply taken into account using measured Al/Si ratios in C–S–H, as thermodynamic models to calculate the Al-uptake by C–S–H are not available. The uptake of alkalis by C–S–H was approached by using an ideal solid solution model between jennite-, tobermorite-like C–S–H, $[(KOH)_{2.5}SiO_2H_2O]_{0.2}$ and $[(NaOH)_{2.5}SiO_2H_2O]_{0.2}$ as proposed by Kulik et al. [114].

A.3. Thermodynamic modelling of hydrated systems

To predict the stable phase assemblage in a hydrated system, assumptions on the degree of reaction of the anhydrous phases have to be made, if possible based on measurements of the specific binders or alternatively based on literature data. For the calculations presented in this paper, where the influence of the presence of different quantities of SiO_2 or fly ash on the hydrate assemblage is modelled, a complete reaction of the Portland cement has been assumed. This assumption was made as we are interested in the long-term composition and as more than 80% Portland cement clinker will have reacted after 28 days or longer (e.g. [1]). For silica-rich SCMs, however, such an assumption is maybe not valid as they react much slower so that even after very long hydration at ambient temperature only a fraction of the silica-rich material will have reacted (for a detailed discussion of the different factors affecting the kinetic of reaction, see above). At higher temperature, however, a higher degree of reaction of the silica-rich material will be achieved.

References

[1] H.F.W. Taylor, Cement Chemistry, Thomas Telford Publishing, London, 1997.
[2] I.G. Richardson, G.W. Groves, The incorporation of minor and trace elements into calcium silicate hydrates (C–S–H) gel in hardened cement pastes, Cement and Concrete Research 23 (1993) 131–138.
[3] H.F.W. Taylor, Nanostructure of C–S–H: current status, Advances in Cement Based Materials 1 (1993) 38–46.
[4] X. Pardal, I. Pochard, A. Nonat, Experimental study of Si–Al substitution in calcium–silicate–hydrate (C–S–H) prepared under equilibrium conditions, Cement and Concrete Research 39 (2009) 637–643.
[5] J.J. Chen, J.J. Thomas, H.F.W. Taylor, H.M. Jennings, Solubility and structure of calcium silicate hydrate, Cement and Concrete Research 34 (2004) 1499–1519.
[6] X. Cong, R.J. Kirkpatrick, ^{29}Si MAS NMR study of the structure of calcium silicate hydrate, Advances in Cement Based Materials 3 (1996) 144–156.
[7] P. Yu, R.J. Kirkpatrick, B. Poe, P.F. McMillan, X. Cong, Structure of calcium silicate hydrate (C–S–H): near-, mid-, and far-infrared spectroscopy, Journal of the American Ceramic Society 82 (3) (1999) 742–748.
[8] H. Minard and J. Skibsted personal communication.
[9] A.V. Girao, I.G. Richardson, R. Taylor, R.M.D. Brydson, Composition, morphology and nanostructure of C–S–H in 70% white Portland cement–30% fly ash blends hydrated at 55 °C, Cement and Concrete Research 40 (2010) 1350–1359.
[10] J.I. Escalante-Garcia, J.H. Sharp, The chemical composition and microstructure of hydration products in blended cements, Cement & Concrete Composites 26 (2004) 967–976.
[11] I.G. Richardson, G.W. Groves, The structure of the calcium silicate phases present in hardened pastes of white Portland cement/blast-furnace slag belnds, Journal of Materials Science 32 (18) (1997) 4793–4802.
[12] R. Taylor, I.G. Richardson, R.M.D. Brydson, Composition and microstructure of 20-year-old ordinary Portland cement–ground granulated blast-furnace slag blends containing 0 to 100% slag, Cement and Concrete Research 40 (7) (2010) 971–983.

[13] V. Kocaba (2009) Development and evaluation of methods to follow microstructural development of cementitious systems including slags. Thesis EPFL No 4523, Lausanne, Switzerland: 263 p pp.
[14] B. Lothenbach, G. Le Saout, E. Gallucci, K. Scrivener, Influence of limestone on the hydration of Portland cements, Cement and Concrete Research 38 (6) (2008) 848–860.
[15] S.-Y. Hong, F.P. Glasser, Alkali binding in cement pastes. Part I. The C—S–H phase, Cement and Concrete Research 29 (1999) 1893–1903.
[16] S.-Y. Hong, F.P. Glasser, Alkali sorption by C–S–H and C–A–S–H gels. Part II. Role of alumina, Cement and Concrete Research 32 (7) (2002) 1101–1111.
[17] J.A. Larbi, A.L.A. Fraay, J.M.J.M. Bijen, The chemistry of the pore fluid of silica fume-blended cement systems, Cement and Concrete Research 20 (1990) 506–516.
[18] J. Duchesne, M.A. Bérubé, The effectiveness of supplementary cementing materials in suppressing expansion due to ASR: another look at the reaction mechanisms. Part 2: pore solution chemistry, Cement and Concrete Research 24 (2) (1994) 221–230.
[19] C. Cau-dit-Coumes, S. Courtois, D. Nectoux, S. Leclercq, X. Bourbon, Formulating a low-alkalinity, high resistance and low-heat concrete for radioactive waste repositories, Cement and Concrete Research 36 (2006) 2152–2163.
[20] M. Codina, C. Cau-dit-Coumes, P. Le Bescop, J. Verdier, J.P. Ollivier, Design and characterization of low heat and low-alkalinity cements, Cement and Concrete Research 38 (2008) 437–448.
[21] E. Schäfer, Einfluss der Reaktion verschiedener Zementhauptbestandteile auf den Alkalihaushalt der Porenlösung des Zementsteins, Verlag Bau + Technik GmbH, Düsseldorf, Germany, 2006, p. 179.
[22] G. Le Saout, E. Lécolier, A. Rivereau, H. Zanni, Chemical structure of cement aged at normal and elevated temperatures and pressures. Part II. Low permeability class G oilwell cement, Cement and Concrete Research 36 (2006) 428–433.
[23] H. Cheng-yi, R.F. Feldman, Hydration reactions in Portland cement–silica fume blends, Cement and Concrete Research 15 (1985) 585–592.
[24] H. Cheng-yi, R.F. Feldman, Influence of silica fume on the microstructural development in cement mortars, Cement and Concrete Research 15 (1985) 285–294.
[25] J.L. Garcia Calvo, A. Hidalgo, C. Alonso, L. Fernandez Luco, Development of low-pH cementitious materials for HLRW repositories. Resistance against ground waters aggression, Cement and Concrete Research 40 (8) (2010) 1290–1297.
[26] B. Lothenbach, Thermodynamics and hydration of blended cement, 2010, CONMOD 2010. Lausanne.
[27] B. Lothenbach, E. Wieland, D. Rentsch, R. Figi and B. Schwyn (in preparation) Hydration of blended cements. Cement and Concrete Research.
[28] T.T.H. Bach (2010) Evolution physico-chimique des liants bas pH hydrates. Influence de la temperature et mécanisme de retention des alcalins. Thesis Université de Bourgogne, Dijon, France: 236 pp.
[29] D.P. Bentz, O.M. Jensen, A.M. Coats, F.P. Glasser, Influence of silica fume on diffusivity in cement-based materials I. Experimental and computer modeling studies on cement pastes, Cement and Concrete Research 30 (6) (2000) 953–962.
[30] X. Luo, D.D.L. Chung, Concrete–concrete pressure contacts under dynamic loading, studied by contact electrical resistance measurement, Cement and Concrete Research 30 (2) (2000) 323–326.
[31] S. Ouellet, B. Bussière, M. Aubertin, M. Benzaazoua, Microstructural evolution of cemented paste backfill: mercury intrusion porosimetry test results, Cement and Concrete Research 37 (12) (2007) 1654–1665.
[32] R. Loser, B. Lothenbach, A. Leemann, M. Tuchscnmid, Chloride resistance of concrete and its binding capacity — comparison between experimental results and thermodynamic modeling, Cement and Concrete Composites 32 (1) (2010) 34–42.
[33] K.O. Kjellsen, E.H. Atlassi, Pore structure of cement silica fume systems — presence of hollow-shell pores, Cement and Concrete Research 29 (1) (1999) 133–142.
[34] S. Hanehara, F. Tomosawa, M. Kobayakawa, K.R. Hwang, Effects of water/powder ratio, mixing ratio of fly ash, and curing temperature on pozzolanic reaction of fly ash in cement paste, Cement and Concrete Research 31 (1) (2001) 31-19.
[35] F.P. Glasser, M. Tyrer, K. Quillin, D. Ross, J. Pedersen, K. Goldthorpe, D.G. Bennett, M. Atkins, The chemistry of blended cements and backfills intended for use in radioactive waste disposal, UK Environment Agency Technical Report P98, 1998.
[36] T.D. Dyer, R.K. Dhir, Hydration reactions of cement combinations containing vitrified incinerator fly ash, Cement and Concrete Research 34 (2004) 849–856.
[37] K.A. Snyder, P.E. Stutzman, J. Philip, D. Esh, Hydrated phases in blended cementitious systems for nuclear infrastructure, Longterm Performance of Cementitious Barriers and Reinforced Concrete in Nuclear Power Plants and Waste Management — NUCPERF 2009, RILEM, Cadarache, France, 2009, pp. 91–98.
[38] K. Luke, E. Lachowski, Internal composition of 20-year-old fly ash and slag-blended ordinary Portland cement pastes, Journal of the American Ceramic Society 91 (12) (2008) 4084–4092.
[39] G. Baert (2009) Physico-chemical interactions in Portland cement–(high volume) fly ash binders. Thesis Department of Structural Engineering, Mangel laboratory for Concrete Research, Ghent University, pp.
[40] J.K. Tishmack, J. Olek, S. Diamond, S. Sahu, Characterization of pore solutions expressed from high-calcium fly-ash-water pastes, Fuel 80 (2001) 815–819.
[41] I.G. Richardson, The calcium silicate hydrates, Cement and Concrete Research 38 (2) (2008) 137–158.
[42] A.M. Harrisson, N.B. Winter, H.F.W. Taylor, An examination of some and composite Portland cement pastes using scanning electron microscopy with X-ray capability, 8th ICCC, 1986, pp. 170–175.
[43] H.S. Pietersen (1993) Reactivity of fly ash and slag in cement. Thesis Delft University of Technology, Delft, The Netherlands: 282 pp.
[44] M. Atkins, F.P. Glasser, A. Kindness, Phase relation and solubility modelling in the $CaO–SiO_2–Al_2O_3–MgO–SO_3–H_2O$ system: for application to blended cements, Material Research Society Symposium Proceedings 212 (1991) 387–394.
[45] I. Pane, W. Hansen, Investigation of blended cement hydration by isothermal calorimetry and thermal analysis, Cement and Concrete Research 35 (2005) 1155–1164.
[46] J.I. Escalante-Garcia, L.Y. Gomez, K.K. Johal, G. Mendoza, H. Mancha, J. Méndez, Reactivity of blast-furnace slag in Portland cement blends hydrated under diffrent conditions, Cement and Concrete Research 31 (2001) 1403–1409.
[47] I.G. Richardson, G.W. Groves, The structure of the calcium silicate hydrate phases present in hardened pastes of white Portland cement blast-furnace slag blends, Journal of Materials Science 32 (18) (1997) 4793–4802.
[48] I.G. Richardson, The nature of C–S–H in hardened cements, Cement and Concrete Research 29 (8) (1999) 1131–1147.
[49] W.A. Gutteridge, J.A. Dalziel, Filler cement: the effect of the secondary component on the hydration of Portland cement: part I. A fine non-hydraulic filler, Cement and Concrete Research 20 (5) (1990) 778–782.
[50] W.A. Gutteridge, J.A. Dalziel, Filler cement: the effect of the secondary component on the hydration of Portland cement: part 2: fine hydraulic binders, Cement and Concrete Research 20 (6) (1990) 853–861.
[51] J. Hjorth, J. Skibsted, H.J. Jakobsen, 29Si MAs NMR studies of Portland cement components and effects of microsilica on the hydration reaction, Cement and Concrete Research 18 (1988) 789–798.
[52] H. Justness, in: P. Colombet, et al., (Eds.), Kinetics of reaction in cementitious pastes containing silica fume as studied by ^{29}Si MAS NMR, Nuclear Magnetic Resonance Spectroscopy of Cement-Based Materials, Springer, Berlin, 1998, pp. 245–267.
[53] R. Fernandez Lopez (2009) Calcined clayey soils as a potential replacemnt for cement in developing countries. Thesis EPFL No 4302, Lausanne, Switzerland: 153 p pp.
[54] J.J. Thomas, J.J. Biernacki, J.W. Bullard, S. Bishnoi, J.S. Dolado, G.W. Scherer, A. Luttge, Modeling and simulation of cement hydration kinetics and microstructure development, Cement and Concrete Research 411 (12) (2011) 1257–1278, (this issue).
[55] S. Bishnoi, K.L. Scrivener, Studying nucleation and growth kinetics of alite hydration using [mu]ic, Cement and Concrete Research 39 (10) (2009) 849–860.
[56] V. Kocaba private communication.
[57] A. Kumar private communication.
[58] G. Le Saout, K. Scrivener, Early hydration of Portland cement with corundum addition, 16. Internationale Baustofftagung (ibausil). Weimar, Germany, 2006, pp. 409–416.
[59] R.J. Detwiler, P.K. Mehta, Chemical and physical effects of silica fume on the mechanical properties of concrete, ACI Materials Journal 86 (6) (1989) 609–614.
[60] C.A. Utton, M. Hayes, J. Hill, N.B. Milestone, J.H. Sharp, Effect of temperatures up to 90 °C on the early hydration of Portland–blastfurnace slag cements, Journal of the American Ceramic Society 91 (3) (2008) 948–954.
[61] X. Wu, D.M. Roy, C.A. Langton, Early stage hydration of slag cement, Cement and Concrete Research 13 (2) (1983) 277–286.
[62] K. Luke, F.P. Glasser, Selectve dissolution of hydrated blast furnace slag cements, Cement and Concrete Research 17 (2) (1987) 273–282.
[63] M. Ben Haha, K. De Weerdt, B. Lothenbach, Quantification of the degree of reaction of fly ash, Cement and Concrete Research 40 (11) (2010) 1620–1629.
[64] A. Gruskovnjak, B. Lothenbach, F. Winnefeld, B. Münch, S.C. Ko, M. Adler, U. Mäder, Quantification of hydration phases in super sulphated cements: review and new approaches, Advances in Cement Research 41 (3) (2010) 279–291.
[65] V. Kocaba, E. Gallucci and K. Scrivener (submitted for publication) Methods for determination of degree of reaction of slag in blended cement pastes. Cement and Concrete Research.
[66] J.S. Lumley, R.S. Gollop, G.K. Moir, H.F.W. Taylor, Degrees of reaction of the slag in some blends with Portland cement, Cement and Concrete Research 26 (1) (1996) 139–151.
[67] M.H. Shehata, M.D.A. Thomas, Use of ternary blends containing silica fume and fly ash to suppress expansion due to alkali–silica reaction in concrete, Cement and Concrete Research 32 (3) (2002) 341–349.
[68] S.K. Antiohos, V.G. Papadakis, E. Chaniotakis, S. Tsimas, Improving the performance of ternary blended cements by mixing different types of fly ashes, Cement and Concrete Research 37 (6) (2007) 877–885.
[69] K. De Weerdt, M. Ben Haha, G. Le Saout, K.O. Kjellsen, H. Justness, B. Lothenbach, Hydration mechanisms of ternary Portland cements containing limestone powder and fly ash, Cement and Concrete Research 41 (3) (2010) 279–291.
[70] K. Scrivener, H.H. Patel, P.L. Pratt and L.J. Parrott (1987) Analysis of phases in cement paste using backscattered electron images, methanol adsorption and thermogravimetric analysis. Microstructural Development during the Hydration of Cement (Proc. Mat. Res. Soc. Symp., 85). Boston, USA: (Proc. Mat. Res. Soc. Symp., 85). 67–76.
[71] K. Scrivener, Backscattered electron imaging of cementitious microstructures: understanding and quantification, Cement and Concrete Composites 26 (2004) 935–945.
[72] X. Feng, E.J. Garboczi, D.P. Bentz, P.E. Stutzman, T.O. Mason, Estimation of the degree of hydration of blended cement pastes by a scanning electron microscope point-counting procedure, Cement and Concrete Research 34 (10) (2004) 1787–1793.
[73] A. Brough, A. Atkinson, Sodium silicate-based, alkali-activated slag mortars part I. Strength, hydration and microstructure, Cement and Concrete Research 32 (6) (2002) 865–879.

[74] C. Porteneuve, J.P. Korb, D. Petit, H. Zanni, Structure–texture correlation in ultra-high-performance concrete — a nuclear magnetic resonance study, Cement and Concrete Research 32 (1) (2002) 97–101.
[75] H.S. Pietersen, A.P.M. Kentgens, G.H. Nachtegaal, W.S. Veeman, J.M.J.M. Bijen, Wet-shotcrete for refractory castables, Proc. 4th International Conference on Fly Ash, Silica Fume, Slag and Natural Pozzolans in Concrete, 1992, pp. 795–812, Istanbul, Turkey: CANET/ACI SP-132-47.
[76] S.L. Poulsen (2009) Methodologies for measuring the degree of reaction in Portland cement blends with supplementary cementitious materials by 29Si and 27Al MAS NMR spectroscopy. Thesis Department of Chemistry and Interdisciplinary Nanoscience Center, Aarhus University, Aarhus, Denmark: 209 pp.
[77] S.L. Poulsen, H.J. Jakobsen, J. Skibsted, Methodologies for measuring the degree of reaction in Portland cement blends with supplementary cementitious materials by ^{27}Al and ^{29}Si MAS NMR spectroscopy, 17. Internationale Baustofftagung (ibausil). Weimar, Germany, 2009, pp. 177–188.
[78] H.M. Dyson, I.G. Richardson, A. Brough, A combined ^{29}Si NMR and selective dissolution technique for the quantitative evaluation of hydrated blast furnace slag cement blends, Journal of the American Ceramic Society 90 (2007) 598.
[79] F. Brunet, T. Charpentier, C.N. Chao, H. Peycelon, A. Nonat, Characterization by solid-state NMR and selective dissolution techniques of anhydrous and hydrated CEM V cement pastes, Cement and Concrete Research 40 (2) (2010) 208–219.
[80] B.B. Sabir, S. Wild, J. Bai, Metakaolin and calcined clays as pozzolans for concrete: a review, Cement & Concrete Composites 23 (2001) 441–454.
[81] B.R. Bickmore, K.L. Nagy, A.K. Gray, A.R. Brinkerhoff, The effect of $Al(OH)_4^-$ on the dissoltion rate of quartz, Geochimica et Cosmochimica Acta 70 (2006) 290–305.
[82] P.M. Dove, The dissolution kintics of quartz in sodiumchloride solutions at 25° to 300 °C, American Journal of Science 294 (1994) 665–712.
[83] R.S. Barneyback, S. Diamond, Expression and analysis of pore fluids of hardened cement pastes and mortars, Cement and Concrete Research 11 (1981) 279–285.
[84] B. Lothenbach, F. Winnefeld, Thermodynamic modelling of the hydration of Portland cement, Cement and Concrete Research 36 (2) (2006) 209–226.
[85] L.Y. Gómez-Zamorano, J.-I. Escalante-García, Effect of curing temperature on the nonevaporable water in Portland cement blended with geothermal silica waste, Cement & Concrete Composites 32 (2010) 603–610.
[86] J. Skibsted, O.M. Jensen, H.J. Jakobsen, Hydration kinetics for the alite, belite, and calcium aluminate phase in Portland cements from ^{27}Al and ^{29}Si MAS NMR spectroscopy, 10th International congress on the chemistry of cement, , 1997, p. 2ii056., Göteborg: Amarkai AB and Congrex Göteborg AG.
[87] J. Duchesne, M.A. Bérubé, Evaluation of the validity of the pore solution expression method from hardened cement pastes and mortars, Cement and Concrete Research 24 (3) (1994) 456–462.
[88] A. Leemann, G. Le Saout, F. Winnefeld, D. Rentsch, B. Lothenbach, Alkali–silica reaction — the influence of calcium on silica dissolution and the formation of reaction products, Journal of the American Ceramic Society 94 (4) (2011) 1243–1249.
[89] L. Lam, Y.L. Wong, C.S. Poon, Degree of hydration and gel/space ratio of high volume fly ash/cement systems, Cement and Concrete Research 30 (2000) 747–756.
[90] E. Sakai, S. Miyahara, S. Ohsawa, S.-H. Lee, M. Daimon, Hydration of fly ash cement, Cement and Concrete Research 35 (2005) 1135–1140.
[91] V.G. Papadakis, Effect of fly ash on Portland cement systems. Part I: low-calcium fly ash, Cement and Concrete Research 29 (1999) 1727–1736.
[92] V.G. Papadakis, Effect of fly ash on Portland cement systems. Part II: high-calcium fly ash, Cement and Concrete Research 30 (2000) 1647–1654.
[93] Rasheeduzzafar, E.S. Hussain, Effect of microsilica and blast furnace slag on pore solution composition and alkali–silica reaction, Cement & Concrete Composites 13 (1991) 219–225.
[94] S. Diamond, Effects of two danish flyashes on alkali contents or pore solutions of cement–flyash pastes, Cement and Concrete Research 11 (1981) 383–394.
[95] F.P. Glasser, K. Luke, M.J. Angus, Modification of cement pore fluid compositions by pozzolanic additives, Cement and Concrete Research 18 (2) (1988) 165–178.
[96] P. Lorenzo, S. Goñi, S. Hernandez, A. Guerrero, Effect of fly ashes with high alkali content on the alkalinity of the pore solution of hydrated Portland cement paste, Journal of the American Ceramic Society 79 (2) (1996) 470–474.
[97] S. Goñi, M.P. Lorenzo, A. Guerrero, M.S. Hernández, Calcium hydroxide saturation factors in the pore solution of hydrated Portland cement fly ash pastes, Journal of the American Ceramic Society 79 (4) (1996) 1041–1046.
[98] M.H. Shehata, M.D.A. Thomas, R.F. Bleszynski, The effects of fly ash composition on the chemistry of pore solution in hydrated cement pastes, Cement and Concrete Research 29 (12) (1999) 1915–1920.
[99] M.H. Shehata, M.D.A. Thomas, Alkali release characteristics of blended cements, Cement and Concrete Research 36 (2006) 1166–1175.
[100] P. Longuet, L. Burglen, A. Zelwer, La phase liquide du ciment hydraté, Revue des matériaux de construction 676 (1973) 35–41.
[101] C. Vernet, E. Démoulian, P. Gourdin, F. Hawthorn, Kinetics of slag cements hydration, 7th International Congress on the Chemistry of Cement, III, 1980, pp. 128–133.
[102] C. Vernet, Comportement de l'ion S– au cours de l'hydratation des ciments riche en laitier (CLK), Silicates industriels 47 (1982) 85–89.
[103] R.F. Bleszynski, R.D. Hooton, M.D.A. Thomas, C.A. Rogers, Durability of ternary blend concretes with silica fume and blastfurnace slag: laboratory and outdoor exposure site studies, ACI Materials Journal 99 (5) (2002) 499–508.
[104] I. Juel, D. Herfort, R. Gollop, J. Konnerup-Madsen, H.J. Jakobsen, J. Skibsted, A thermodynamic model for predicting the stability of thaumasite, Cement & Concrete Composites 25 (2003) 867–872.
[105] E.P. Nielsen, D. Herfort, M.R. Geiker, Phase equilibria of hydrated Portland cement, Cement and Concrete Research 35 (2005) 109–115.
[106] B. Lothenbach, T. Matschei, G. Möschner, F.P. Glasser, Thermodynamic modelling of the effect of temperature on the hydration and porosity of Portland cement, Cement and Concrete Research 38 (1) (2008) 1–18.
[107] T. Matschei, B. Lothenbach, F.P. Glasser, The role of calcium carbonate in cement hydration, Cement and Concrete Research 37 (4) (2007) 551–558.
[108] D. Kulik, GEMS-PSI 2.3, available at http://www.gems.web.psi.ch/ 2009, PSI-Villigen, Switzerland.
[109] W. Hummel, U. Berner, E. Curti, F.J. Pearson and T. Thoenen, Nagra/PSI Chemical Thermodynamic Data Base 01/01. 2002, USA, also published as Nagra Technical Report NTB 02-16, Wettingen, Switzerland: Universal Publishers/uPUBLISH.com. 565.
[110] T. Thoenen, D. Kulik, Nagra/PSI chemical thermodynamic database 01/01 for the GEM-Selektor (V.2-PSI) geochemical modeling code, 2003, PSI TM-44-02-09.
[111] T. Matschei, B. Lothenbach, F.P. Glasser, Thermodynamic properties of Portland cement hydrates in the system $CaO–Al_2O_3–SiO_2–CaSO_4–CaCO_3–H_2O$, Cement and Concrete Research 37 (10) (2007) 1379–1410.
[112] D.A. Kulik, M. Kersten, Aqueous solubility diagrams for cementitious waste stabilization systems: 4. A carbonation model for Zn-doped calcium-silicate hydrate by Gibbs energy minimization, Environmental Science & Technology 36 (2002) 2926–2931.
[113] D.A. Kulik, M. Kersten, Aqueous solubility diagrams for cementitious waste stabilization systems: II, end-member stoichiometries of ideal calcium silicates hydrate solid solutions, Journal of the American Ceramic Society 84 (12) (2001) 3017–3026.
[114] D. Kulik, J. Tits, E. Wieland, Aqueous–solid solution model of strontium uptake in C–S–H phases, Geochimica et Cosmochimica Acta 71 (12, Supplement 1) (2007) A530.